1-1-2013

Novel receiver for correlated fading multi-antenna physical network coding TWRNs

Le Chung Tran
University of Wollongong, lctran@uow.edu.au

A. Mertins
University of Wollongong, mertins@uow.edu.au

Peter James Vial
University of Wollongong, peterv@uow.edu.au

Vinh Van Nguyen
Hung Yen University of Technology And Education, vinhnv.utehy@gmail.com

Novel receiver for correlated fading multi-antenna physical network coding TWRNs

Abstract

Physical Network Coding (PNC) has recently been proposed for multi-antenna Two-Way Relay Networks (TWRNs) with independent fading channels because the total network throughput could be significantly improved. However, PNC for multi-antenna TWRNs with correlated fading channels has not been considered yet. This paper thus considers an important class of multi-antenna TWRNs with the following properties: single-antenna source nodes and two-antenna relay; distance between source nodes and the relay is significantly larger than that between antennas of the relay; and channels between source nodes and the relay are correlated. For such a system, we first propose a novel correlation model that facilitates an easy method to create fading channels with certain correlation properties. We then propose an ovelreceiver design for correlated fading TWRNs. Simulation results show that the proposed receiver design provides much better error performance than the well-known Log-Likelihood Ratio (LLR) algorithm proposed in the literature.

Keywords

fading, coding, multi, twrns, correlated, antenna, receiver, physical, novel, network

Disciplines

Engineering | Science and Technology Studies

Publication Details

L. Chung. Tran, A. Mertins, P. James. Vial & V. Van. Nguyen, "Novel receiver for correlated fading multi-antenna physical network coding TWRNs," Advances in Communication Technology, vol. 5, pp. 16-25, 2013.

Novel Receiver for Correlated Fading Multi-Antenna Physical Network Coding TWRNs

Le Chung Tran[1,a] , Alfred Mertins[2,b], Peter James Vial[1,a] and Vinh Van Nguyen[3,c]

[1]University of Wollongong, Australia
[2]University of Luebeck, Germany
[3]Hung Yen University of Technology & Education, Vietnam

[a] {lctran,peterv}@uow.edu.au, [b] mertins@isip.uni-luebeck.de, [c] vinhnv.utehy@gmail.com

Keywords: Physical network coding, Two-Way Relay Network, multiple antennas, correlated fading.

Abstract. Physical Network Coding (PNC) has recently been proposed for multi-antenna Two-Way Relay Networks (TWRNs) with independent fading channels because the total network throughput could be significantly improved. However, PNC for multi-antenna TWRNs with correlated fading channels has not been considered yet. This paper thus considers an important class of multi-antenna TWRNs with the following properties: single-antenna source nodes and two-antenna relay; distance between source nodes and the relay is significantly larger than that between antennas of the relay; and channels between source nodes and the relay are correlated. For such a system, we first propose a novel correlation model that facilitates an easy method to create fading channels with certain correlation properties. We then propose a novel receiver design for correlated fading TWRNs. Simulation results show that the proposed receiver design provides much better error performance than the well-known Log-Likelihood Ratio (LLR) algorithm proposed in the literature.

Introduction

Network coding (NC) has been proposed in the literature to improve the throughput of wireless sensor networks, wireless ad-hoc networks, wireless multicast and broadcast networks. To examine these networks, bi-directional relaying or two-way relay networks (TWRNs) are used as a basic model where information is exchanged between source nodes in both directions. TWRNs have been intensively examined, such as in [1]– [2]. There are three main transmission protocols, namely conventional protocol, network coding, and physical network coding (PNC), for TWRNs as depicted in Fig. 1(a). The conventional protocol involves totally four time slots (or phases), while network coding [2]–[5] involves only three phases. In network coding, original bits q_1 and q_2 from source nodes must be individually decoded before the message $q_3 = q_1 \oplus q_2$ can be created. PNC is the most efficient protocol in terms of maximizing the total throughput of the network since it only involves two steps, given that channels between nodes are half-duplex and the same radio carrier frequency is used by all nodes in the TWRN[4]. In PNC [6]–[10], the original bits q_1 and q_2 are not recovered. Instead, the message $q_3 = q_1 \oplus q_2$ is directly estimated based on the sum of the noisy signals received by the relay from two source nodes (the superimposed signal). The waveform x_3 corresponding to the message q_3 can be created directly from the superimposed waveform $x_1 + x_2$, based on a certain physical network mapping algorithm. Since adding the waveforms and mapping this sum to the waveform x_3 can be done directly in the PHY layer.

[4]If channels are full-duplex, i.e. nodes can transmit and receive signals simultaneously, e.g. over different frequency bands such as in multiband-OFDM ultra-wideband systems [11]–[13], the conventional and NC protocols might require as few as two steps, eliminating the difference in the number of time slots between all three protocols.

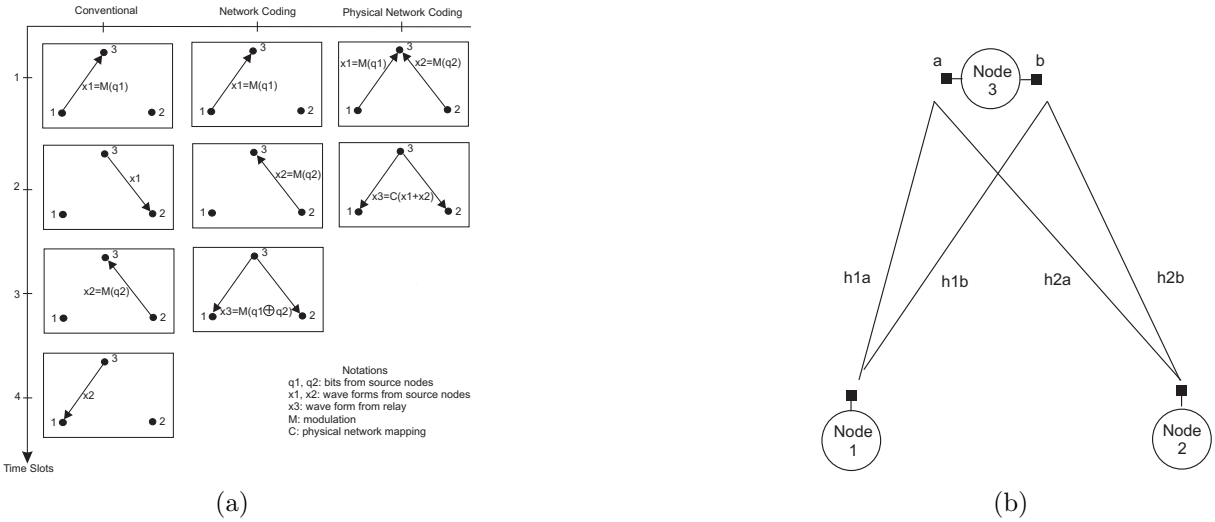

(a) (b)

Fig. 1: (a) Three transmission protocols for TWRNs; (b) Multi-antenna TWRN with correlated fading channels.

Although PNC has been intensively examined, correlation between fading channels has not been considered in all aforementioned works. Examples of channel correlation include, but are not limited to, the correlation of fading channels between a) a base station in a mobile cellular network and two mobile users; between two antennas of a base station and an individual mobile user; b) Earth station and multiple antennas of the satellite in a satellite communications system; c) a satellite and two end users in a terrestrial mobile satellite communications system; and d) two WLAN (wireless local area network) equipments and their access point. Note that two end-users might not be able to communicate directly with each other, but via the relay, even when the two users are relatively close to each other (thus correlation exits), compared to the relay, due to, for instance, the authorization, security, or confidential issues. Channel correlation could significantly degrade the performance of TWRNs.

Given that PNC for multi-antenna TWRNs or for truly MIMO TWRNs has received increasing attention, a convenient mathematical correlation model and an efficient physical network mapping technique for correlated fading TWRNs are specially desired. An efficient detection algorithm for TWRNs with correlated fading channels seems to be missing in the literature. Therefore, in this paper, we first derive a novel mathematical model for channel correlation in TWRNs, which facilitates not only an easy way to generate correlated fading channels corresponding to certain correlation properties, but also the derivation of our novel detection technique for PNC in multi-antenna TWRNs with correlated fading channels.

The paper starts with the derivation of a mathematical model for channel correlation in TWRNs. Based on this model, a novel receiver design is proposed for PNC TWRNs in correlated fading channels, followed by two case studies for correlated TWRNs and insightful discussions over these cases. Simulation results are then provided. The conclusion concludes the paper.

System Model of Correlated TWRNs

We consider a multi-antenna TWRN in Fig. 1(b) where Nodes 1 and 2 are the source nodes with one antenna each, and Node 3 is the relay equipped with two antennas a and b. This is an important class of generally defined MIMO TWRNs since each source node might only be equipped with a single antenna, rather than multiple antennas, due to its portable, tiny size. Denote h_{ik} and d_{ik}, $i \in \{1, 2\}, k \in \{a, b\}$, to be the complex channel coefficients and the distances between Node i and the k-th antenna of Node 3, respectively. We emphasize an important property of a TWRN with physical network coding that the source nodes transmit/receive

signals on the *same radio carrier frequency* at the *same time* to/from the relay. Further to this fact, we assume that

- Distance d_{ik} ($i \in \{1,2\}$, $k \in \{a,b\}$) is significantly larger than the distance d_{12} between Node 1 and Node 2, and much larger than the distance d_{ab} between two antennas of Node 3. Consequently, $d_{1a} \approx d_{1b}$, $d_{2a} \approx d_{2b}$. An typical example is a satellite system, where Node 3 is the satellite and Nodes 1 and 2 are two terrestrial mobile users or two nearby Earth stations;
- There exists correlation between all channel coefficients h_{ik} in the network;
- Channels are reciprocal and are (block) flat Rayleigh fading channels.

Given the above fact and assumptions, it is reasonable to assume that

- Energies of the channels between Node 1 and two antennas of Node 3 are equal, i.e. $|h_{1a}| = |h_{1b}|$. Small difference in their magnitudes (e.g. due to small-scaled fading effects) is considered to be negligible.
- The phase difference between h_{1a} and h_{1b} (e.g. due to the small difference between d_{1a} and d_{1b}, or small-scaled fading effects) is necessary to be considered. Thus we write $h_{1b} = e^{j\theta_1}h_{1a}$, where h_{1a} is assumed to follow $\mathcal{CN}(0,1)$, and θ_1 is an uniform random variable (RV) following the distribution $\mathcal{U}[\theta_{1\min}, \theta_{1\max}]$.
- Similarly, energies of the channels between Node 2 and two antennas of Node 3 are assumed to be identical, while their phase difference is non-negligible. Thus we could write $h_{2b} = e^{j\theta_2}h_{2a}$, where $\theta_2 \sim \mathcal{U}[\theta_{2\min}, \theta_{2\max}]$.
- Energy of the channels between Nodes 2 and 3 might be different from that of the channels between Nodes 1 and Node 3 (e.g. due to the difference between the distances d_{1k} and d_{2k}), resulting in non-negligible differences in their large-scaled (e.g. shadowing) and small-scaled fading effects. This energy difference shall be presented by a factor r (r is a positive real number) between $|h_{2a}|$ and $|h_{1a}|$, i.e. $|h_{2a}| = r|h_{1a}|$. Both scenarios where r is either a constant or a RV are considered in this paper.
- Beside, the phase difference between h_{2a} and h_{1a} might also exist, i.e. $h_{2a} = re^{j\theta_3}h_{1a}$, where $\theta_3 \sim \mathcal{U}[\theta_{3\min}, \theta_{3\max}]$.

As a result, the correlated channels could be presented by the following relations

$$h_{1b} = e^{j\theta_1}h_{1a},\ h_{2b} = e^{j\theta_2}h_{2a},\ h_{2a} = re^{j\theta_3}h_{1a}. \tag{1}$$

If $|h_{1a}|$ is a Rayleigh distributed RV and r is a constant, it is easy to realize $|h_{1b}|$, $|h_{2a}|$ and $|h_{2b}|$ are also Rayleigh RVs. Further, these channels are mutually correlated. Particularly, from (1), we have $h_{2b} = re^{j(\theta_2+\theta_3-\theta_1)}h_{1b} := re^{j\theta_4}h_{1b}$, where $\theta_4 := \theta_2 + \theta_3 - \theta_1$. It is possible to prove that θ_4 can be approximated by a Gaussian RV. Specially, if θ_1, θ_2, and θ_3 follow the distribution $\mathcal{U}[-\pi/2, \pi/2]$, then $\theta_4 \sim \mathcal{N}(0, 2.47)$. (The proof is not mentioned here due to the limited space. Instead, the probability distribution function and histogram of the sum of three uniform RVs each of which follows $\mathcal{U}[-\pi/2, \pi/2]$ is presented in Fig. 2(a) for illustration).

If we denote θ to be a uniformly distributed RV within the range $[\theta_{\min},\ \theta_{\max}]$, v a complex Gaussian RV $v \sim \mathcal{CN}(0,1)$, $z := e^{j\theta}$, and $w := e^{j\theta}v$, then the expected value $E\{z\}$ is

$$E\{z\} = \frac{e^{j\theta_{\max}} - e^{j\theta_{\min}}}{j(\theta_{\max} - \theta_{\min})}. \tag{2}$$

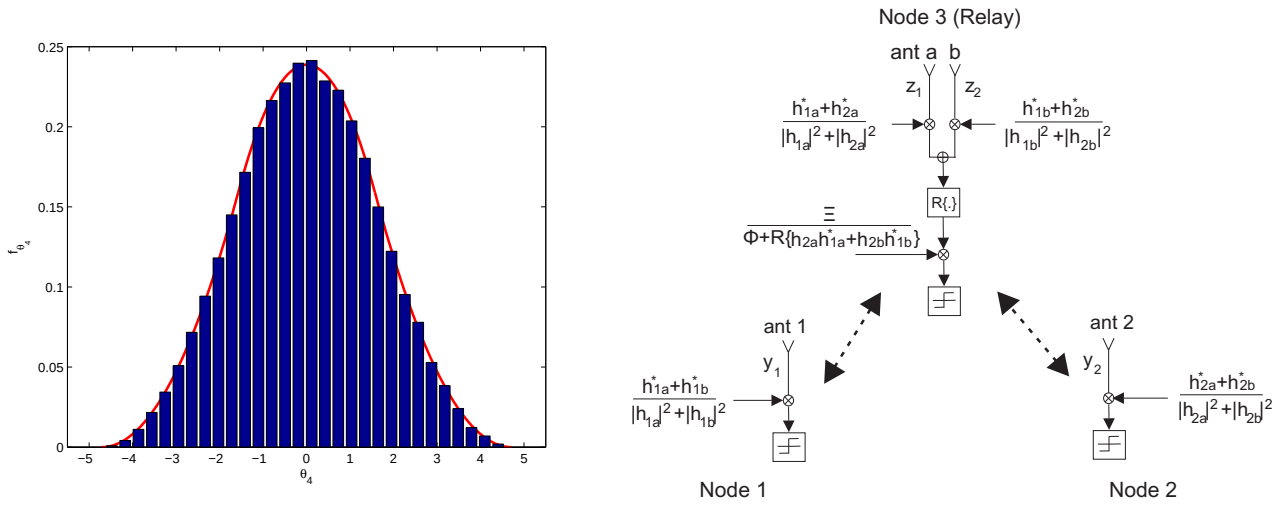

(a) (b)

Fig. 2: (a) Probability distribution function (solid curve) and histogram of θ_4; (b) Proposed MRC-like receivers for source nodes and relay node in correlated fading TWRNs.

Since $v \sim \mathcal{CN}(0,1)$, we have $E\{v\} = E\{v^*\} = 0$ and $\text{var}\{v\} = 1$. Further

$$E\{w\} = E\{ve^{j\theta}\} = E\{v\}E\{e^{j\theta}\} = 0, \tag{3}$$

because v and θ are mutually independent. Therefore

$$\text{var}\{w\} = E\{ww^*\} - E\{w\}E\{w^*\} = E\{vv^*\} = 1. \tag{4}$$

Correlation coefficient between w and v is defined as

$$\rho(w,v) = \left| \frac{E\{wv^*\} - E\{w\}E\{v^*\}}{\sqrt{\text{var}(w)\text{var}(v)}} \right|. \tag{5}$$

From (3), (4), and (5), we have

$$\rho(w,v) = |E\{wv^*\}| = |E\{ve^{j\theta}v^*\}| = |E\{vv^*\}E\{e^{j\theta}\}| = |E\{e^{i\theta}\}|. \tag{6}$$

From (2) and (6), we can write

$$\rho(w,v) = \left| \frac{\sqrt{(\cos\theta_{\max} - \cos\theta_{\min})^2 + (\sin\theta_{\max} - \sin\theta_{\min})^2}}{\theta_{\max} - \theta_{\min}} \right|. \tag{7}$$

Thus two RVs v and $w = ve^{j\theta}$ have the same expected and variance values, and their correlation is presented by the correlation coefficient in (7). Similarly, for $w = rve^{j\theta}$, where r is a positive real coefficient, we have $E\{w\} = 0$ and $\text{var}\{w\} = r^2$. The correlation between v and w is still presented by the correlation coefficient in (7).

Applying (7), the correlation coefficients between the pairs of channels (h_{1a}, h_{1b}), (h_{2a}, h_{2b}), and (h_{1a}, h_{2a}) are calculated as

$$\rho_l = \left| \frac{\sqrt{(\cos\theta_{l\max} - \cos\theta_{l\min})^2 + (\sin\theta_{l\max} - \sin\theta_{l\min})^2}}{\theta_{l\max} - \theta_{l\min}} \right| \tag{8}$$

for $l \in \{1,2,3\}$, respectively. Specially, if $\theta_{l\max} = -\theta_{l\min}$, (8) turns into

$$\rho_l = \left| \frac{\sin(\theta_{l\max})}{\theta_{l\max}} \right| = |\text{sinc}(\theta_{l\max})|, \tag{9}$$

By adjusting $\theta_{l\min}$ and $\theta_{l\max}$, the mutual correlation coefficients between channels can be adjusted, and hence the desired correlation coefficients can be easily achieved.

Meanwhile, if we denote $\theta_4 \sim \mathcal{N}(0, \sigma_{\theta_4}^2)$, it is possible to prove that the correlation coefficient between (h_{1b}, h_{2b}) is calculated as

$$\rho_4 = |e^{j\mu_{\theta_4} + \frac{1}{2}j^2\sigma_{\theta_4}^2}| = |e^{-\frac{1}{2}\sigma_{\theta_4}^2 + j\mu_{\theta_4}}|. \tag{10}$$

The novel presentation of correlated fading channels in the considered TWRN as mentioned in (1) allows us to derive a novel detection technique for this multi-antenna physical network coding TWRN in correlated fading channels as below.

MRC-Like Receiver For Correlated TWRNs

We denote x_1 and x_2 to be the modulated signals transmitted from Nodes 1 and 2 respectively. BPSK modulation is used for the illustration of the proposed concept. Thus the possible values of x_1 and x_2 are ± 1. Received signals at the receive antennas of Node 3 are written as

$$z_a = h_{1a}x_1 + h_{2a}x_2 + w_a, \quad z_b = h_{1b}x_1 + h_{2b}x_2 + w_b,$$

where w_a and w_b are noise terms affecting the antennas a and b of Node 3. We consider the following term

$$T = \underbrace{\frac{z_a\left(h_{1a}^* + h_{2a}^*\right)}{|h_{1a}|^2 + |h_{2a}|^2}}_{T_1} + \underbrace{\frac{z_b\left(h_{1b}^* + h_{2b}^*\right)}{|h_{1b}|^2 + |h_{2b}|^2}}_{T_2}, \tag{11}$$

where $(.)^*$ denotes the complex conjugate. We will then calculate the real part of the expectation value $E\{T\}$, denoted as $\Re\{E\{T\}\}$, with respect to (w.r.t) h_{ik}. If noise terms are omitted, T_1 can be written as

$$T_1 := \frac{P_1}{Q_1} = \frac{\left(h_{1a}x_1 + h_{2a}x_2\right)\left(h_{1a}^* + h_{2a}^*\right)}{|h_{1a}|^2 + |h_{2a}|^2} + w_{T_1} = \frac{|h_{1a}|^2x_1 + |h_{2a}|^2x_2 + h_{2a}h_{1a}^*x_2 + h_{2a}^*h_{1a}x_1}{|h_{1a}|^2 + |h_{2a}|^2} + w_{T_1}, \tag{12}$$

where P_1 and Q_1 present the numerator and denominator which are bivariate non-independent RVs w.r.t h_{ik}, and $w_{T_1} = \frac{w_a\left(h_{1a}^* + h_{2a}^*\right)}{|h_{1a}|^2 + |h_{2a}|^2}$. It is well-known that $E\{T_1\} = E\left\{\frac{P_1}{Q_1}\right\} \neq \frac{E\{P_1\}}{E\{Q_1\}}$ even if P_1 and Q_1 are independent RVs. Specifically, $E\{T_1\}$ can be estimated (see Eq.(4) in [14]) by a second-order Taylor expansion around $E\{P_1\}$ and $E\{Q_1\}$ as follows

$$E\left\{\frac{P_1}{Q_1}\right\} \approx \frac{E\{P_1\}}{E\{Q_1\}} - \frac{\mathrm{cov}\{P_1, Q_1\}}{(E\{Q_1\})^2} + \frac{\mathrm{var}\{Q_1\}E\{P_1\}}{(E\{Q_1\})^3} \tag{13}$$

Because Q_1 is a positive real RV, we have

$$\mathrm{cov}\{P_1, Q_1\} = E\{(P_1 - E\{P_1\})(Q_1 - E\{Q_1\})^*\} = E\{P_1Q_1\} - E\{P_1\}E\{Q_1\} \tag{14}$$

For illustration, we assume the channel coefficients follow Eq.(1), $h_{1a} \sim \mathcal{CN}(0, 1)$, and $\theta_l \sim \mathcal{U}[-\theta_{l\min}, \theta_{l\max}]$ for $l \in [1, 2, 3]$. We could prove that

$$E\{Q_1\} = 2, \quad E\{P_1\} = x_1 + x_2 + E\{e^{i\theta_3}\}x_2 + E\{e^{-i\theta_3}\}x_1,$$
$$E\{P_1Q_1\} = 4E\{P_1\}. \tag{15}$$

From (14) and (15), we have

$$\mathrm{cov}\{P_1, Q_1\} = 4E\{P_1\} - 2E\{P_1\} = 2E\{P_1\}. \tag{16}$$

Table 1: Mapping from $x_1 + x_2$ to $q_1 \oplus q_2$.

q_1	q_2	x_1	x_2	$x_1 + x_2$	$q_1 \oplus q_2$
0	0	1	1	2	0
0	1	1	-1	0	1
1	0	-1	1	0	1
1	1	-1	-1	-2	0

Substitute (15) and (16) into (13), we have

$$E\{T_1\} \approx \frac{E\{P_1\}}{E\{Q_1\}} - \frac{2E\{P_1\}}{4} + \frac{4E\{P_1\}}{8} = \frac{E\{P_1\}}{E\{Q_1\}} \tag{17}$$

Clearly, from (17), $E\{T_1\}$ can be well approximated by $\frac{E\{P_1\}}{E\{Q_1\}}$ when T_1 is defined in (12) although, in general, $E\{T_1\} \neq E\{P_1\}/E\{Q_1\}$.

Denote

$$\Phi = E\{|h_{1a}|^2 + |h_{1b}|^2\} \tag{18}$$

$$\Psi = E\{h_{2a}h_{1a}^*\}; \;\; \Omega = E\{h_{2b}h_{1b}^*\}, \tag{19}$$

where Φ is a positive real number and Ψ, Ω are complex numbers. Further, if the following conditions are satisfied

$$E\{|h_{1a}|^2 + |h_{1b}|^2\} = E\{|h_{2a}|^2 + |h_{2b}|^2\}, \tag{20}$$

$$E\{|h_{1a}|^2 + |h_{2a}|^2\} = E\{|h_{1b}|^2 + |h_{2b}|^2\} = \Xi, \tag{21}$$

where Ξ is a positive real number, and given x_1 and x_2, from (17), we will have

$$E\{T_1\} \approx \frac{E\{|h_{1a}|^2x_1 + |h_{2a}|^2x_2 + h_{2a}h_{1a}^*x_2 + h_{2a}^*h_{1a}x_1\}}{E\{|h_{1a}|^2 + |h_{2a}|^2\}} = \frac{E\{|h_{1a}|^2x_1 + |h_{2a}|^2x_2\}}{\Xi} + \frac{\Psi x_2 + \Psi^* x_1}{\Xi}. \tag{22}$$

Note that the condition (20) shall be guaranteed if channels follow (1) with $r = 1$, but not strictly guaranteed if $r \neq 1$. Both scenarios will be discussed in more detail in Section .

Similarly, we can write $E\{T_2\}$ in (11) as

$$E\{T_2\} \approx \frac{E\{|h_{1b}|^2x_1 + |h_{2b}|^2x_2\}}{\Xi} + \frac{\Omega x_2 + \Omega^* x_1}{\Xi} \tag{23}$$

From (22) and (23), we have

$$E\{T\} = E\{T_1\} + E\{T_2\} \approx \frac{\Phi(x_1 + x_2) + (\Psi + \Omega)x_2 + (\Psi + \Omega)^* x_1}{\Xi}.$$

This results in

$$\Re\{E\{T\}\} = \frac{\left[\Phi + \Re\{(\Psi + \Omega)\} \quad\right]}{\Xi}(x_1 + x_2).$$

Alternatively, the superimpose waveform is

$$x_1 + x_2 = \frac{\Xi\Re\{E\{T\}\}}{\Phi + \Re\{(\Psi + \Omega)\}}. \tag{24}$$

From (24), by releasing the expectation operation in $E\{T\}$, Ψ and Ω, to account for the instantaneous channel coefficient, we propose the estimate of $(x_1 + x_2)$ as follows

$$\widehat{x_1 + x_2} = \frac{\Xi\Re\{T\}}{\Phi + \Re\{h_{2a}h_{1a}^* + h_{2b}h_{1b}^*\}}, \tag{25}$$

where T is calculated by (11), and Φ and Ξ are calculated by (18) and (21) respectively.

If q_1 (q_2) denotes the original binary bit transmitted from Node 1 (Node 2) then, unlike the conventional NC where q_1 and q_2 must be completely recovered from x_a and x_b at the relay before the message $q_3 = q_1 \oplus q_2$ is broadcasted to Nodes 1 and 2, in PNC, $q_3 = q_1 \oplus q_2$ is formed directly from $\widehat{x_1 + x_2}$. Table I shows the mapping from the superimposed signal $x_1 + x_2$ to $q_1 \oplus q_2$. Clearly, this is a multi-to-one mapping (e.g. $\widehat{x_1 + x_2} = 2$ and $\widehat{x_1 + x_2} = -2$ might be both mapped to $q_3 = 0$). Note that multi-to-one mapping is a well-known drawback of PNC.

We propose the following simple mapping rule

$$q_1 \oplus q_2 = \begin{cases} 0, & \text{if } |\widehat{x_1 + x_2}| > \Upsilon; \\ 1, & \text{otherwise.} \end{cases}$$

For the ease of comparison, the threshold Υ is selected to be the same as the optimal threshold in the well-known LLR (Log-Likelihood Ratio) method [6], $\Upsilon = 1 + \frac{N_0}{2} \ln(1 + \sqrt{1 - e^{-4/N_0}})$, where N_0 is the noise variance ($\Upsilon = 1.3443$ for $N_0 = 1$). In other words, the BPSK signal x_3 should be directly created based on the following proposed mapping rule

$$x_3 = \begin{cases} +1, & \text{if } |\widehat{x_1 + x_2}| > \Upsilon; \\ -1, & \text{otherwise.} \end{cases}$$

where $\widehat{x_1 + x_2}$ is calculated by (25). The BPSK signal x_3 will be now broadcasted through the antennas a and b of Node 3 to Nodes 1 and 2. Since channels are reciprocal and block flat fading, the channel coefficients from these antennas to Nodes 1 and 2 are still assumed to be h_{1a}, h_{2a}, h_{1b} and h_{2b}. Received signals at Nodes 1 and 2 can be written as

$$z_1 = h_{1a}x_3 + h_{1b}x_3 + w_1, \quad z_2 = h_{2a}x_3 + h_{2b}x_3 + w_2.$$

The estimate of x_3, denoted as $\hat{x}_3$, will be created at Node 1 (Node 2) based on the following MRC (Maximum Ratio Combining) rule

$$\hat{x}_3 = \frac{z_1(h_{1a}^* + h_{1b}^*)}{|h_{1a}|^2 + |h_{1b}|^2} \quad \left(\text{or } \hat{x}_3 = \frac{z_2(h_{2a}^* + h_{2b}^*)}{|h_{2a}|^2 + |h_{2b}|^2} \right) \tag{26}$$

The MRC-like detecting algorithms proposed in (11), (25) and (26) is shown more clearly in Fig. 2(b).

The message $q_3 = q_1 \oplus q_2$ will be estimated, denoted as $\widehat{q_1 \oplus q_2}$, by these nodes based on the rule

$$\widehat{q_1 \oplus q_2} = \begin{cases} 0, & \text{if } \hat{x}_3 \geq 0; \\ 1, & \text{otherwise.} \end{cases}$$

Finally, the message q_2 (q_1) transmitted from Node 2 (Node 1) will be received by Node 1 (Node 2) as

$$\hat{q}_1 = q_2 \oplus (\widehat{q_1 \oplus q_2}); \quad \hat{q}_2 = q_1 \oplus (\widehat{q_1 \oplus q_2})$$

The above analysis has been derived for a two-antenna relay. Generation for a multi-antenna relay is straightforward.

Case Studies and Discussions

Case 1: This case considers the channel conditions in (1) with $r = 1$, i.e.

$$h_{1b} = e^{j\theta_1} h_{1a}, \; h_{2b} = e^{j\theta_2} h_{2a}, \; h_{2a} = e^{j\theta_3} h_{1a}, \tag{27}$$

and θ_1, θ_2 and θ_3 being independent uniform RVs following the distribution $\mathcal{U}[-\pi/2, \pi/2]$. Note that the below analysis also holds for an arbitrary range $[\theta_{l\min},\ \theta_{l\max}]$, for $l \in [1, 2, 3]$.

From (27), we have

$$h_{2a}h_{1a}^* = e^{j\theta_3},\ h_{2b}h_{1b}^* = e^{j(\theta_3+\theta_2-\theta_1)}. \tag{28}$$

In our simulation, $h_{1a} \sim \mathcal{CN}(0, 1)$. From (18), (21) and (27), we have $\Phi = \Xi = 2$. The proposed estimate (25) becomes

$$\widehat{x_1 + x_2} = \frac{2\Re\{T\}}{[2 + \cos(\theta_3) + \cos(\theta_3 + \theta_2 - \theta_1)]}$$

Discussion: Practically, the conditions (27) mean the differences in magnitudes of channel coefficients due to small-scaled fading effects are negligible, and only phase differences are considered. The phase differences between each pair of channel coefficients are totally arbitrary. A reasonable example is a satellite system where the distances from Node 3 to Nodes 1 and 2 are significantly larger than both the distances between two antennas at Node 3 and between Nodes 1 and 2. In such a system, the distances d_{ik} ($i \in \{1, 2\}$, $k \in \{a, b\}$) can be considered to be roughly equal. It is recalled that, although Nodes 1 and 2 might be closer to each other, compared to the relay, as the general assumption of network coding, these two nodes cannot communicate directly with each other (e.g. due to obstruction, security, and/or network administration issues).

Case 2: We consider more generalized channel conditions as follows

$$h_{1b} = e^{j\theta_1}h_{1a},\ h_{2a} = re^{j\theta_3}h_{1a},\ h_{2b} = e^{j\theta_2}h_{2a} = re^{j(\theta_3+\theta_2)}h_{1a}, \tag{29}$$

where $\theta_l \sim \mathcal{U}[-\pi/2, \pi/2]$ for $l \in [1, 2, 3]$ and r is an arbitrary positive real number. In this case, if $r \neq 1$, the condition (20) does not hold anymore since

$$|h_{1a}|^2 + |h_{1b}|^2 = 2|h_{1a}|^2; \quad |h_{2a}|^2 + |h_{2b}|^2 = 2r^2|h_{1a}|^2.$$

The difference between these two terms is presented by the term Δ defined as

$$\Delta = \left|\frac{(|h_{2a}|^2 + |h_{2b}|^2) - (|h_{1a}|^2 + |h_{1b}|^2)}{|h_{1a}|^2 + |h_{1b}|^2}\right| = |r^2 - 1|.$$

The term Δ is referred to as the mismatch factor hereafter. Equivalently, we have $r = \sqrt{1 \pm \Delta}$. Without loss of generality, we could assume that $r > 1$, i.e. the energies of the channels between Node 2 and Node 3 are assumed to be greater than those between Node 1 and Node 3, if $\Delta > 0$. Alternatively, r can be calculated as

$$r = \sqrt{1 + \Delta}. \tag{30}$$

Discussion: Unlike *Case 1*, channel coefficients in (29) might have different magnitudes and phases. A reasonable example could be a satellite system, where d_{ik} are significantly larger than the antenna spacing d_{ab} at Node 3, and than the distances between Nodes 2 and 3, d_{2k} ($k \in \{a, b\}$), are considerably different from those between Nodes 1 and 3, d_{1k}. In such a system, it is reasonable to assume that $|h_{1a}| \approx |h_{1b}|$, $|h_{2a}| \approx |h_{2b}|$ within the channel coherent time window, thus if $|h_{2a}| = r|h_{1a}|$, then $|h_{2b}| = r|h_{1b}|$. The difference in the phases of the pair h_{1a} and h_{1b} (or h_{2a} and h_{2b}) exists, while the difference in the magnitudes of this pair is neglected. Clearly, this is a more generalized scenario than *Case 1*. Since the estimate (25) is derived assuming that the condition (20) is guaranteed (i.e. $r = 1$ strictly), the estimate shall perform poorer in this case, compared to the case $r = 1$. Different values of Δ will be used to present different mismatch levels in the condition (20) and the tolerance and robustness of the proposed estimate will be evaluated accordingly via simulations.

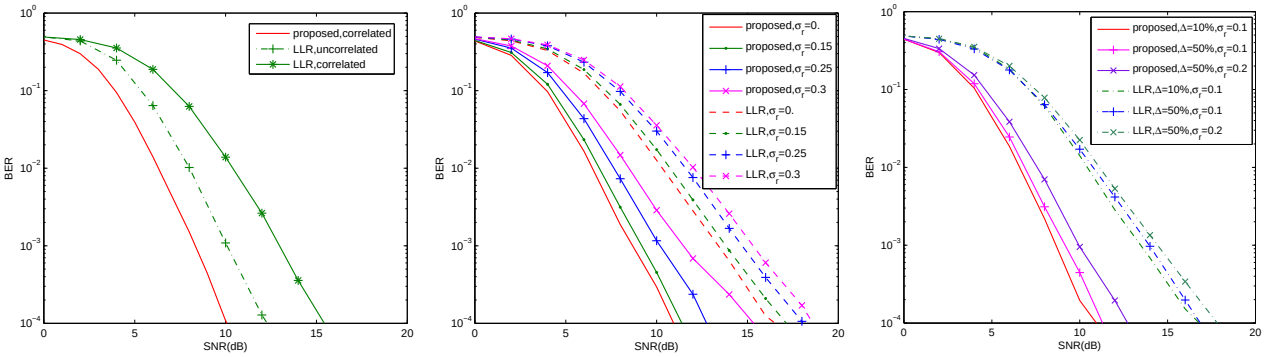

(a) (b) (c)

Fig. 3: Proposed algorithm vs. LLR [6]. Correlated channels are created based on (a) Eq.(27); (b) Eq.(29) with a fixed mismatch factor $\Delta = 30\%$ and r is a random variable; and (c) Eq.(29) with different mismatch conditions and r is a random variable.

Simulation Results

To illustrate the efficiency of the proposed mapping algorithm, Monte-Carlo simulations are run for 10,000 binary bits transmitted from each source node over each among 100 channel realizations. Channel coding used at nodes is a rate-1/2 convolutional encoder.

Fig. 3(a) presents the performances of the proposed mapping technique and of the well-known LLR method [6] in both cases of completely independent channels as well as correlated channels following (27) (i.e. $r = 1$, $\Delta = 0$). While the LLR method (dotted curve) works relatively well in the case of independent channels, it performs poorly in the case of correlated channels (marked solid curve). This is simply because the LLR method was not derived for the case of correlated fading channels. The proposed MRC-like algorithm, on the contrary, performs extremely well in this scenario. Its performance is even better than that of the LLR method in the case of independent channels by approximate 2dB.

Fig. 3(b) presents the performance of the proposed algorithm when channel coefficients are correlated following (29). The mismatch factor Δ is assumed to be 30%, while r is a real Gaussian RV (rather than a constant $r = 1$), $r \sim \mathcal{N}(\bar{r}, \sigma_r^2)$, where $\bar{r}$ is calculated by (30) (i.e. $\bar{r} = 1.14$ for $\Delta = 30\%$). The standard deviation values $\sigma_r = 0$, 0.15, 0.25, and 0.3 are considered. Clearly, the proposed algorithm still outperforms the LLR algorithm in the same channel conditions, though the former is slightly more sensitive to σ_r than the latter.

Similarly to Fig. 3(b), Fig. 3(c) illustrates the proposed algorithm in comparison with the LLR method in correlated fading channels (29). However, different combinations of the pair of mismatch level Δ (10% or 50%) and standard deviation σ_r (0.1 or 0.2) are considered. It is shown that, although the proposed estimate (25) is derived based on the condition (20) (i.e. $\Delta = 0$ - the total energy of the channels between Nodes 2 and 3 is assumed to be the same as that between Nodes 1 and 3), the proposed algorithm is still very robust, compared to LLR, even when this condition is not strictly guaranteed.

Conclusions

This paper examines TWRNs with: a) single-antenna source nodes and multi-antenna relay; b) the distances between the source nodes and the antennas of the relay being significantly larger than that between the antennas of the relay; and c) channels being reciprocal and block flat Rayleigh fading ones and correlation existing between these channels. For such networks, we have proposed for the first time the correlation model between fading channels, which

facilitates not only an easy way to generate correlated fading channels with certain correlation coefficients, but also our derivation of a novel receiver design which outperforms the well-known LLR algorithm [6]. Our future work would be the modification of the proposed algorithm to tailor for higher density modulation constellations and for truly MIMO TWRNs.

References

[1] C. E. Shannon: *Two-way communication channels*, University of California Press, vol. 1 (1961), pp. 611–644.

[2] B. Rankov and A. Wittneben: *Spectral efficient protocols for half-duplex fading relay channels*, IEEE Journal on Selected Areas in Communications, vol. 25, no. 2 (2007), pp. 379 –389.

[3] S. Katti, H. Rahul, H. Wenjun, D. Katabi, M. Medard, and J. Crowcroft: *Xors in the air: Practical wireless network coding*, IEEE/ACM Transactions on Networking, vol. 16, no. 3 (2008), pp. 497–510.

[4] S. Kim and J. Chun: *Network coding with linear MIMO pre-equalizer using modulo in two-way channel*, IEEE International Wireless Communications and Network Conference (2008), pp. 517 –521.

[5] H.-Q. Lai and K.J.T. Liu: *Space-time network coding*, IEEE Transation on Signal Processing, vol. 59, no. 4 (2011), pp. 1706 –1718.

[6] S. Zhang, S. C. Liew, and P. P. Lam: *Hot topic: physical-layer network coding*, 12th Annual Int. Conf. Mobile Computing and Netw. (2006), pp. 358–365.

[7] P. Popovski and H. Yomo: *Physical network coding in two-way wireless relay channels*, IEEE Int. Conf. Commun. (2007), pp. 707 –712.

[8] S. Zhang and S. C. Liew: *Physical layer network coding with multiple antennas*, IEEE Wireless Communications and Networking Conference (2010), pp. 1 –6.

[9] S. Ogawa and F. Ono; *STBC-MIMO network coding with dual polarization antennas*, 20th IEEE Int. Conf. Comp. Commun. Netw. (2011), pp. 1–6.

[10] S. L. Zhang, L. Lu, C. Nie, G. Qian, and F. Wang: *Channel coding and decoding in a MIMO TWRC with physical-layer network coding*, 23rd IEEE Int. Symp. Personal Indoor and Mobile Radio Commun. (2012), pp. 95 –99.

[11] W. Abbott et. al.: *Multiband OFDM physical layer specification*, (WiMedia Alliance Release 1.5 2009).

[12] L. C. Tran and A. Mertins: *Space-time frequency code implementation in MB-OFDM UWB communications: design criteria and performance*, IEEE Trans. Wireless Commun., vol. 8, no. 2 (2009), pp. 701–713.

[13] L. C. Tran, A. Mertins, and T. A. Wysocki: *Unitary differential space-time-frequency codes for MB-OFDM UWB wireless communications*, IEEE Trans. Wireless Commun. vol. 12, no. 2 (2013), pp. 862-876.

[14] G.M.P. van Kempen and L.J. van Vliet: *Mean and variance of ratio estimators used in fluorescence ratio imaging*, Journal of the International Society for Advancement of Cytometry, vol. 39, no. 4 (2000), pp. 300–305.